NASA TECHNICAL MEMORANDUM

NASA TM X-1619

NASA TM X-1619

COLD FLOW INVESTIGATION OF A LOW ANGLE TURBOJET PLUG NOZZLE WITH FIXED THROAT AND TRANSLATING SHROUD AT MACH NUMBERS FROM 0 TO 2.0

by Donald L. Bresnahan and Albert L. Johns

Lewis Research Center
Cleveland, Ohio

NATIONAL AERONAUTICS AND SPACE ADMINISTRATION • WASHINGTON, D. C. • AUGUST 1968

NASA TM X-1619

COLD FLOW INVESTIGATION OF A LOW ANGLE TURBOJET PLUG NOZZLE WITH FIXED THROAT AND TRANSLATING SHROUD AT MACH NUMBERS FROM 0 to 2.0

By Donald L. Bresnahan and Albert L. Johns

Lewis Research Center
Cleveland, Ohio

NATIONAL AERONAUTICS AND SPACE ADMINISTRATION

For sale by the Clearinghouse for Federal Scientific and Technical Information
Springfield, Virginia 22151 – CFSTI price $3.00

ABSTRACT

The performance of a full-length plug nozzle can be maintained at a high level by extending the outer shroud with increases in nozzle pressure ratio from 2.5 to the design pressure ratio of 26.3. During acceleration, maximum external flow effects occurred at Mach 1.5 with performance losses of approximately 2.8 percent. At subsonic cruise, this loss was about 4.8 percent. Plug truncations to one-half and one-third of its full length resulted in losses of 1 and 1.7 percent, respectively, at Mach 2.0. Base bleed of about 1.5 percent of the primary flow optimized the performance of the truncated plugs.

COLD FLOW INVESTIGATION OF A LOW ANGLE TURBOJET PLUG NOZZLE WITH FIXED THROAT AND TRANSLATING SHROUD AT MACH NUMBERS FROM 0 TO 2.0

by Donald L. Bresnahan and Albert L. Johns

Lewis Research Center

SUMMARY

An experimental investigation was conducted in the Lewis Research Center's nozzle static test facility and 8- by 6-Foot Supersonic Wind Tunnel to determine the performance characteristics of a 10^{o} half angle conical turbojet plug nozzle. Its overall design pressure ratio was 26.3. The internal expansion for this fixed throat nozzle was adjusted by translating a cylindrical outer shroud.

The performance of a full-length plug could be maintained at a high level by extending the outer shroud with increases in nozzle pressure ratio from 2.5 to 27. The maximum external flow effects during acceleration occurred at about Mach 1.5 and resulted in a performance loss of approximately 2.8 percent. At subsonic cruise, the external flow effects were as much as 4.8 percent because the nozzle was operating at a low pressure ratio where the external drag became a large percent of the relatively low ideal thrust.

Truncating the plug to approximately one-half and one-third of its full length resulted in performance losses of 1 and 1.7 percent, respectively, at Mach 2.0. Base bleed of about 1.5 percent of the primary flow reduced these losses to 0.7 and 0.9 percent.

INTRODUCTION

As part of a broad program in airbreathing propulsion, the Lewis Research Center is evaluating various nozzle geometries appropriate for supersonic cruise applications. In this continuing program, plug nozzles are receiving considerable emphasis because they may offer the potential of good aerodynamic performance together with a minimum

of complexity and a consequent reduction in maintenance problems. This report documents the aerodynamic performance of a plug nozzle configuration suitable for a non-afterburning turbojet engine designed for cruise at a Mach number near 2.7.

High internal performance can be obtained with isentropic plug nozzles. External flow, however, has an adverse effect on performance of this type of nozzle due to the high base drag and resultant overexpansion losses on the plug surface at off-design pressure ratios resulting from the high lip angles inherent with this design (refs. 1 to 3). Another approach to plug nozzle design is the low angle conical plug with a small boattail angle (ref. 4). This nozzle reduces the base drag and overexpansion effects by reducing the boattail angle. Good subsonic performance is obtained; but for transonic and supersonic operation, it must incorporate a translating shroud to provide internal expansion appropriate to the particular Mach number and its corresponding pressure ratio. Plug nozzles with translating shrouds were studied (ref. 5) for overall design pressure ratios up to 20 and plug half angles of $7\frac{1}{2}^{\circ}$, 10°, and 15°. It was determined a 10° half angle was optimum; however, the variations in pressure ratio and Mach number were rather limited. In practice, the shroud would translate to keep the internal expansion pressure ratio approximately equal to the nozzle pressure ratio. However, the maximum shroud length was determined by the condition at which the initial Mach line from the shroud lip just intercepts the plug tip. At higher pressure ratios, the shroud remains fixed since any further extension adds weight and friction without affecting the plug expansion field. This limiting internal expansion pressure ratio varies with both plug angle and nozzle design pressure ratio. For the 10° half angle plug of reference 5 this ratio was approximately 80 percent of the nozzle design pressure ratio.

This investigation was conducted to determine the performance of a nozzle with a higher design pressure ratio than that reported in reference 5. A 10° half angle plug nozzle with translating shroud and an overall design pressure ratio of 26.3 was tested in the Lewis Research Center's nozzle static test facility and also in the 8- by 6-Foot Supersonic Wind Tunnel at Mach numbers up to 1.97 to determine the external flow effects. Effects of plug truncation to approximately one-half and one-third of the original length were also studied with various amounts of base bleed.

Dry air at room temperature was used for primary and base-bleed flows in both facilities; and maximum nozzle pressure ratios of 27.0 and 22.0 were obtained in the static test facility and the 8- by 6-Foot Supersonic Wind Tunnel, respectively.

SYMBOLS

A area

D drag

d	model diameter
F	thrust
L	full plug length measured from nozzle throat
M	Mach number
P	total pressure
p	static pressure
r	radius
T	total temperature
w	weight flow rate
$\frac{w_b}{w_p}\sqrt{\frac{T_b}{T_p}}$	corrected base-bleed flow rate ratio
x	axial distance measured from nozzle throat
Subscripts	
b	base
bt	boattail
i	ideal
j	jet
max	maximum
p	primary
x	condition at distance x
0	free stream
7	nozzle inlet
8	nozzle throat
9	nozzle exit

APPARATUS AND INSTRUMENTATION

Installation in Static Test Facility

A schematic view of the research hardware installation in the static test facility is shown in figure 1. The nozzles were mounted on a section of pipe which was freely sus-

pended by four flexure rods connected to the bedplate. Pressure forces acting on the nozzle and mounting pipe, both external and internal, were transmitted from the bedplate through a bell crank to a calibrated balanced-air-pressure diaphragm which was used in measuring thrust. A labyrinth seal around the necked-down inlet section ahead of the mounting pipe separated the nozzle-inlet air from the exhaust and provided a means of maintaining a pressure difference across the nozzle. The space between the two labyrinth seals was vented to the test chamber. This decreased the pressure differential across the second labyrinth and prevented a pressure gradient on the outside of the diffuser section due to an air blast from under the labyrinth seal.

Pressures and temperatures were measured at the various stations indicated. Total and wall static pressure measurements were used at the bellmouth inlet to compute inlet momentum and at the primary air-metering station to compute the primary air flow. The nozzle-inlet total pressure and temperature were measured at station 7 and ambient exhaust pressure at station 0.

Installation in 8- by 6-Foot Supersonic Wind Tunnel

A schematic drawing of the model support system in the 8- by 6-Foot Supersonic Wind Tunnel showing the internal geometry and thrust-measuring system is shown in figure 2. The grounded portion of the model was supported from the tunnel ceiling by a vertical strut. The floating portion was attached to the primary and base-bleed air bottles cantilevered by flow tubes from external supply manifolds. The primary air bottle was supported by front and rear bearings. The base-bleed air passed through the plug which was supported by struts attached to the nozzle outer shroud. The axial force of the nozzle, which included base-bleed flow effects, was transmitted to the load cell located in the nose of the model. Since the floating portion of the model included a portion of the afterbody and boattail, the measured force was that resulting from the interaction of the internal and external flows of the nozzle.

A static calibration of the thrust-measuring system was obtained by applying known forces to the nozzle and measuring the output of the load cell. A water-cooled jacket surrounded the load cell and maintained a constant temperature of 90° F to eliminate errors in the calibration due to variations in temperature from aerodynamic heating.

Nozzle Configurations

The nozzle configurations consisted of a 10° half-angle plug with external shrouds of varying lengths to simulate translation. Its overall design pressure ratio was 26.3.

The maximum shroud length was selected to expand the flow to 80 percent of the design pressure ratio internally. Basic nozzle dimensions are shown in figure 3(a). The maximum model diameter was 8.5 inches (21.59 cm) with a circular arc boattail on the shroud to reduce base drag. The shroud base area ratio A_{bt}/A_{max} was arbitrarily selected to be 0.1146. In figure 3(b) are shown the shroud extensions that were tested, and their corresponding design pressure ratios and internal area ratios are listed in table I.

The plug was segmented as shown in figure 3(c) so that truncated plug configurations could be studied.

Photographs of the full-length plug with several shroud lengths are shown in figure 4 and the truncated plug configurations in figure 5.

Nozzle Instrumentation

The primary and base-bleed total pressures were obtained by use of total-pressure probes as shown in figure 6(a). A row of static-pressure orifices was located on the plug at a meridian angle of 180° (fig. 6(b)) with several orifices also located at angles of 0° and 270°. Pressures were also measured at the base of the truncated plugs.

PROCEDURE

Static Test Facility

Pressure ratios were set by maintaining a constant nozzle inlet pressure and varying the exhaust pressure. Each configuration was tested over a range of pressure ratios which were appropriate for the particular shroud extension ratio.

8- by 6-Foot Supersonic Wind Tunnel

Nozzle performance was obtained over a range of pressure ratios at several Mach numbers for each shroud length tested. The nozzle pressure ratio was varied by changing the nozzle inlet pressure. The maximum pressure ratio at each Mach number was restricted due to the limitations of the primary air supply and the ambient pressure at that Mach number. The highest pressure ratio obtained was approximately 22.0 at Mach 1.97. To obtain a realistic simulation of important flight conditions, nozzle pressure ratio was varied at each Mach number around a typical schedule for a supersonic turbojet engine as shown in figure 7.

DATA REDUCTION

Static Test Facility

The nozzle primary air flow was calculated from pressure and temperature measurements in the necked-down section of the mounting pipe and an effective area determined by an ASME calibration nozzle. The base-bleed air flow was measured by means of a standard ASME flow-metering orifice in the external supply line.

Actual jet thrust was calculated from thrust cell measurements corrected for tare forces. The ideal jet thrust for each of the primary and base-bleed flows was calculated from the measured mass flow rate expanded from their measured total pressures to p_0. Provision was made to set the ideal thrust of the bleed flow to zero if the total pressure was less than p_0. Review of the data, however, showed that this situation did not occur for this nozzle. Nozzle efficiency is defined then as the ratio of the actual jet thrust to the ideal thrust of both primary and base-bleed flows.

$$\text{Nozzle static efficiency} = \frac{F_j}{F_{ip} + F_{ib}}$$

8- by 6-Foot Supersonic Wind Tunnel

Both primary and base-bleed flow rates were measured by means of standard ASME flow-metering orifices located in the external supply lines. Thrust-minus-drag measurements were obtained from a load cell readout of the axial forces acting on the floating portion of the model. Internal tare forces, determined by internal areas and measured tare pressures located as shown in figure 2, were accounted for in the thrust calculation.

The only external friction drag charged to the nozzle is that downstream of station 107.55 (273.2 cm), shown in figure 2. That force acting on the portion of the nozzle between station 93.65 (237.9 cm) and 107.55 (273.2 cm) was also measured on the load cell but is not considered to be part of the nozzle drag. Its magnitude was estimated using the semiempirical flat plate mean skin friction coefficient given in figure 7 of reference 6 as a function of free-stream Mach number and Reynolds number. The coefficient accounts for variations in boundary-layer thickness and profile with Reynolds number. Previous measurements of the boundary layer characteristics at the aft end of this jet exit model in the 8- by 6-Foot Supersonic Wind Tunnel indicated that the profile and thickness were essentially the same as that computed for a flat plate of equal length. The strut wake appeared to affect only a localized region near the top of the model and

resulted in a slightly lower local free-stream velocity than measured on the side and bottom of the model. Therefore, the results of reference 6 were used without correction for three-dimensional flow effects or strut interference effects. The resulting correction was applied to the load cell force.

The ideal jet thrust for each of the primary and base-bleed flows was calculated from the measured mass flow rate expanded from their measured total pressures to p_0. Provision was made to set the ideal thrust of the bleed flow to zero if the total pressure was less than p_0. Review of the data, however, showed that this situation did not occur for this nozzle. Nozzle efficiency is defined then as the ratio of the thrust minus drag to the ideal thrust of both primary and base-bleed flows.

$$\text{Nozzle efficiency} = \frac{F - D}{F_{ip} + F_{ib}}$$

RESULTS AND DISCUSSION

Full-Length Plug

Various shroud lengths were tested to simulate shroud translation over a wide range of pressure ratios. The static performance of six shroud lengths is shown in figure 8. With continuous translation of shroud position, peak performance would be maintained over a broad range of pressure ratios. For pressure ratios greater than 15.0, optimum static performance could be obtained with a shroud location $x/d = 0.915$ ($A_9/A_8 = 2.41$).

The effect of external flow on the plug nozzle performance is presented in figure 9. Each shroud was tested over a range of pressure ratios at several Mach numbers as shown. Again it is apparent that a translating shroud is required to provide optimum performance over a broad range of Mach numbers and pressure ratios. The subsonic cruise performance is low since the nozzle is operating at a low pressure ratio off the peak of the performance curve. At these low values of pressure ratio where ideal thrust is relatively low, the external drag becomes a large percent of the ideal thrust.

External flow effects on plug pressure distributions are shown in figure 10 for selected pressure ratios, Mach numbers, and shroud positions. Good agreement was obtained between the two test facilities at $M_0 = 0$. The external flow effects were negligible at most Mach numbers with the greatest effect occurring at Mach 1.47. At this Mach number there was a greater overexpansion on the plug surface with external flow as evidenced by the lower plug pressures (fig. 10(i)).

The effect of external flow on nozzle performance over the full Mach number range is summarized in figure 11. Average static performance obtained with the translating

shroud is indicated by the dashed line. The solid line shows the optimum performance of the shrouds tested based on the operating schedule of figure 7. The maximum external flow effects during acceleration occur at about Mach 1.5 resulting in a 2.8 percent performance loss. The shaded area shows the estimated loss attributed to the friction drag on the external shroud. The cross-hatched area indicates the loss due to increased overexpansion on the plug surface with external flow. This was determined by the differences in the plug force between static and wind-tunnel results and can also be seen in the plug pressure distributions in figure 10. The balance of the performance loss is presumed to be an indication of the boattail drag.

At subsonic cruise, the performance is very sensitive to both pressure ratio and Mach number. The maximum external flow effects occurred at a pressure ratio of 3.25 at Mach 0.9 resulting in approximately a 4.8 percent performance decrement. The nozzle was operating at a low pressure ratio where the external drag became a large percent of the relatively low ideal thrust. As indicated in the figure, increasing the operating pressure ratio schedule assumed to be required for subsonic cruise also increased performance by almost 2 percent. Selecting a lower subsonic cruise Mach number even with a lower pressure ratio also improved performance for this flight condition.

Fifty Percent Plug Length

There is a continuing effort to increase the payload of aircraft by increasing the performance and reducing the weight of engine components. One obvious way to reduce the weight of a plug nozzle would be to shorten the plug. Truncated plugs, therefore, were tested to determine the effect of truncation on the plug nozzle performance. The comparative performance of two shroud positions at several Mach numbers is shown in figure 12. The retracted shroud is for low-pressure ratio operation at takeoff and subsonic cruise, while the extended shroud is for the high-pressure ratios or supersonic cruise. For these conditions, the losses due to truncation were between 1 and 2 percent. This loss may be due to the combined effects of removing part of the expansion surface on which forces were acting, increased divergence losses, and any base drag that may be encountered with the blunt plug base.

The losses resulting from plug truncation may be minimized by increasing the plug base pressure with small amounts of base-bleed flow exiting from the open plug base. The effect of this base bleed on nozzle performance is shown in figure 13 for both the retracted and extended shrouds. Between 1 and 2 percent base bleed results in small increases in performance for the retracted shroud but does not show any noticeable improvement with the extended shroud.

The effect of base bleed on the plug base pressure is shown in figure 14. For the

retracted shroud (fig. 14(a)), the base pressure is near ambient without base bleed and increases slightly with bleed flow. With the shroud extended (fig. 14(b)), the base pressure is below ambient without base bleed and is increased considerably as bleed flow increased. Maximum effects occurred with about 3 percent bleed flow.

Bleed flow pumping characteristic curves for the retracted and extended shroud configurations are shown in figure 15. The pressure recovery needed to supply this base bleed is shown in figure 16. At takeoff, the pumping is poor and bleed flows greater than 1 percent could not be furnished by inlets but would have to come from the engine cycle. With external flow at the subsonic and supersonic speeds shown, the pumping is much improved and bleed flows of 2 to 5 percent could possibly be obtained from inlets.

Thirty Percent Plug Length

The plug length was further reduced to 30 percent and tested with the retracted and extended shrouds. The effect of this truncation is shown in figure 17 where performance losses between 1.7 and 2.8 percent resulted, depending on the operating conditions. The effect of base bleed on nozzle performance is shown in figure 18 where the peak performance with both shroud extensions was obtained with approximately 1.5 percent bleed. With the shorter plug, base bleed has a greater effect because the losses due to truncation are greater. The effect of base bleed on the plug base pressure is shown in figure 19. With the shroud retracted (fig. 19(a)), the base pressure is near ambient without base bleed and increased slightly with increasing bleed flow. For the extended shroud (fig. 19(b)), the base pressure is below ambient without base bleed but increased considerably with bleed flow.

Base bleed pumping characteristic curves for both shroud configurations are given in figure 20. The pressure recovery needed to supply this bleed flow is shown in figure 21. Again pumping at takeoff is very poor, and bleed flows greater than about 0.5 percent could not be furnished by inlets but would have to come from the engine cycle. At the subsonic and supersonic speeds shown, the pumping is much better and bleed flows of 2 to 5 percent could possibly be obtained from inlets.

A summary of the effect of truncation on nozzle performance is shown in figure 22. The retracted shroud is shown for the low-pressure ratio operation at takeoff and subsonic cruise and the extended shroud for the higher pressure ratios at supersonic Mach numbers. There is approximately a 1 percent loss in performance for the 50 percent truncation and between 1.7 and 2.8 percent for the 30 percent plug length. In general, 1.5 percent base bleed gave optimum performance and is indicated by the dashed line. With this amount of bleed, approximately 0.3 to 0.5 of the performance loss due to truncation was regained, depending on configuration and flight condition.

SUMMARY OF RESULTS

An experimental investigation was conducted to determine the external flow effects on the performance characteristics of a 10^{o} half-angle conical turbojet plug nozzle with an overall design pressure ratio of 26.3. The internal expansion was adjusted by translating a cylindrical outer shroud. The following general trends were indicated:

1. A high level of performance can be maintained over a wide range of pressure ratios by translating the shroud to adjust the internal expansion.

2. The maximum external flow effects during acceleration occurred at approximately Mach 1.5 and resulted in a 2.8 percent loss in performance. At subsonic cruise, the external flow effects could result in a performance loss of as much as 4.8 percent because the nozzle operates at a low pressure ratio where the external drag becomes a large percent of the relatively low ideal thrust. The subsonic cruise performance is very sensitive to pressure ratio and Mach number.

3. Truncating the plug to 50 percent resulted in approximately 1 percent performance loss. Further truncation to 30 percent resulted in 1.7 to 2.8 percent loss, depending on flight condition.

4. Approximately 1.5 percent corrected base-bleed flow rate appeared to optimize performance for the truncated plugs examined.

5. The base bleed pumping characteristics for this model were poor for low pressure ratios and no external flow.

Lewis Research Center
National Aeronautics and Space Administration
Cleveland, Ohio, April 18, 1968,
720-03-01-08-22.

REFERENCES

1. Valerino, Alfred S.; Zappa, Robert F.; and Abdalla, Kaleel L.: Effects of External Stream on the Performance of Isentropic Plug-Type Nozzles at Mach Numbers of 2.0, 1.8, and 1.5. NASA Memo 2-17-59E, 1959.

2. Salmi, Reino J.: Preliminary Investigation of Methods to Increase Base Pressure of Plug Nozzles at Mach 0.9. NACA RM E56J05, 1956.

3. Salmi, Reino J.; and Cortright, E. M., Jr.: Effects of External Stream Flow and Afterbody Variations on the Performance of a Plug Nozzle at High Subsonic Speeds. NACA RM E56F11a, 1956.

4. Schmeer, James W.; Kirkham, Frank S.; and Salters, Leland B., Jr.: Performance Characteristics of a 10^{o} Conical Plug Nozzle at Mach Numbers Up to 1.29. NASA TM X-913, 1964.

5. Herbert, M. V.; Golesworthy, G. T.; and Herd, R. J.: The Performance of a Centre Body Propelling Nozzle With a Parallel Shroud in External Flow, Part II. Rep. ARC-CP-894, Aeronautical Research Council, 1966.

6. Smith, K. G.: Methods and Charts for Estimating Skin Friction Drag in Wind Tunnel Tests With Zero Heat Transfer. Rep. ARC-CP-824, Aeronautical Research Council, 1965.

TABLE I. - SHROUD VARIABLES

[Overall design pressure ratio, 26.3.]

Shroud axial length to diameter ratio, x/d	Internal expansion pressure ratio	Internal area ratio,[a] A_9/A_8
1.315	21.30	3.01
.915	14.74	2.41
.515	9.85	1.92
.259	6.05	1.47
.161	4.30	1.26
.087	3.25	1.12

[a]Based on full-length plug.

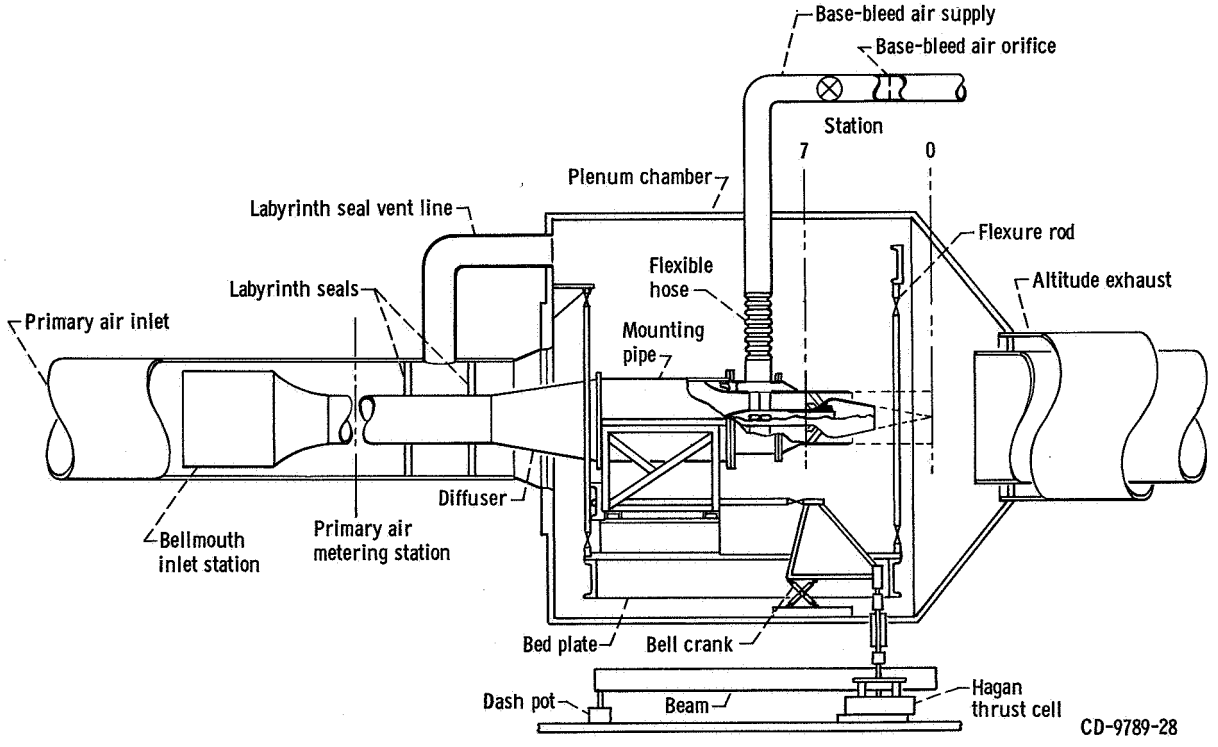

Figure 1. - Schematic view of static test facility.

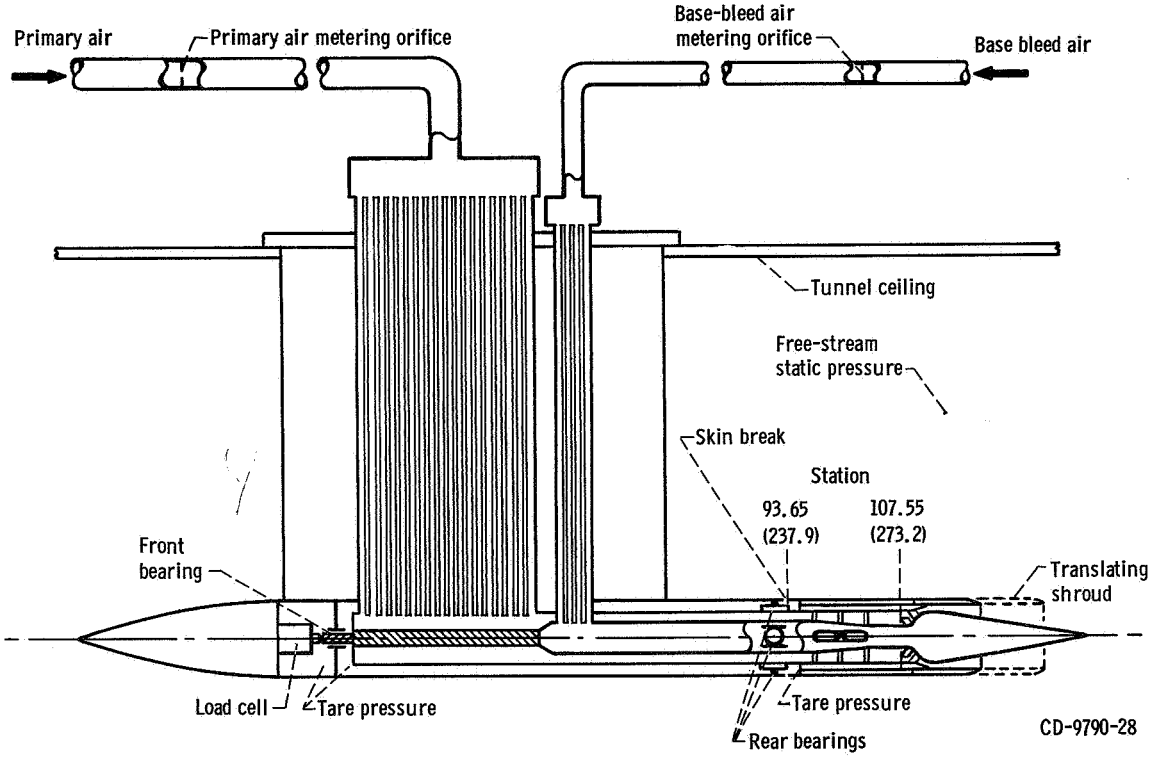

Figure 2. - Nozzle support model and air supply systems. (All dimensions are in inches (cm).)

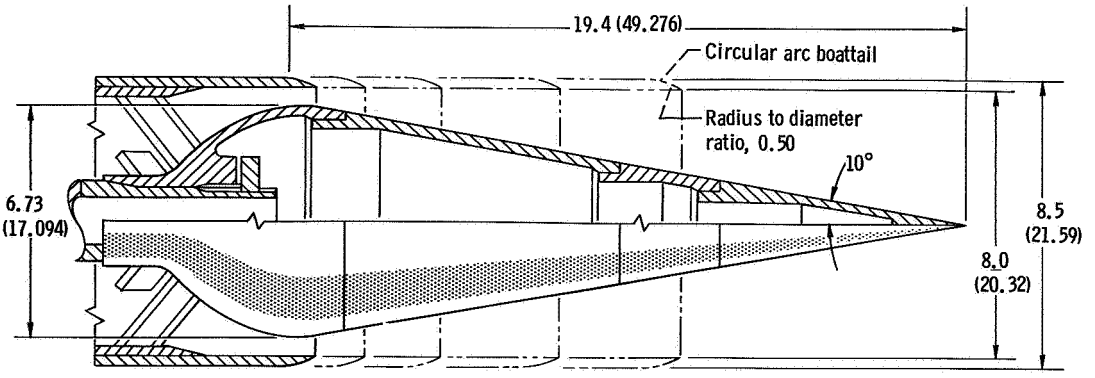

(a) Plug nozzle model dimensions.

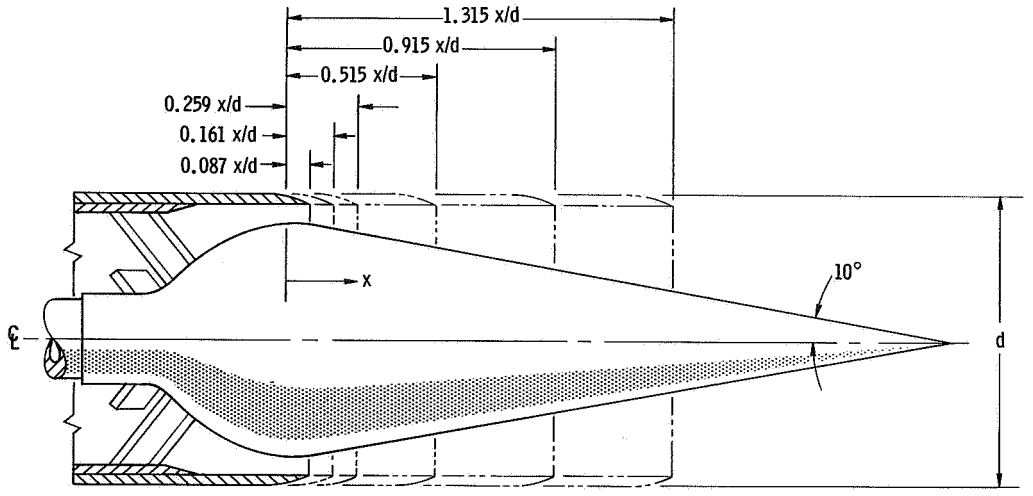

(b) Plug nozzle shroud locations in terms of axial length to diameter ratios. (See table I for design pressure ratios and internal area ratios at these locations.)

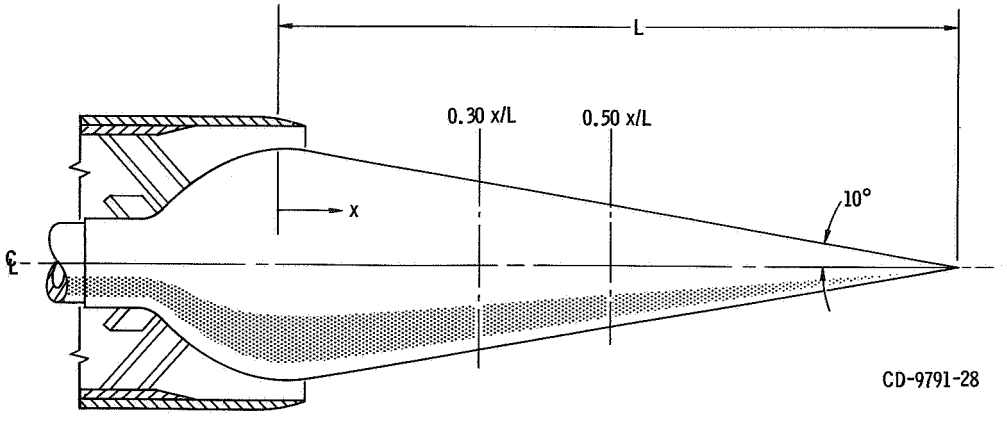

(c) Plug nozzle truncations.

Figure 3. - Model dimensions and geometric variables. (All dimensions are in inches (cm) unless otherwise noted.)

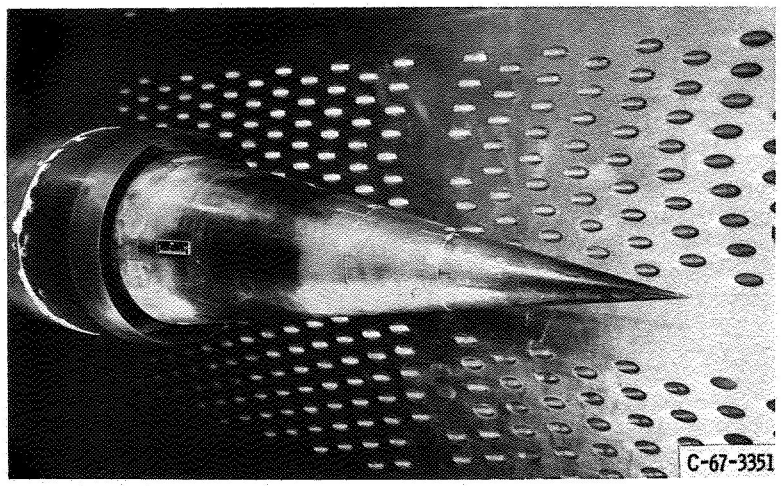

Shroud location: x/d, 0.087; A_9/A_8, 1.12

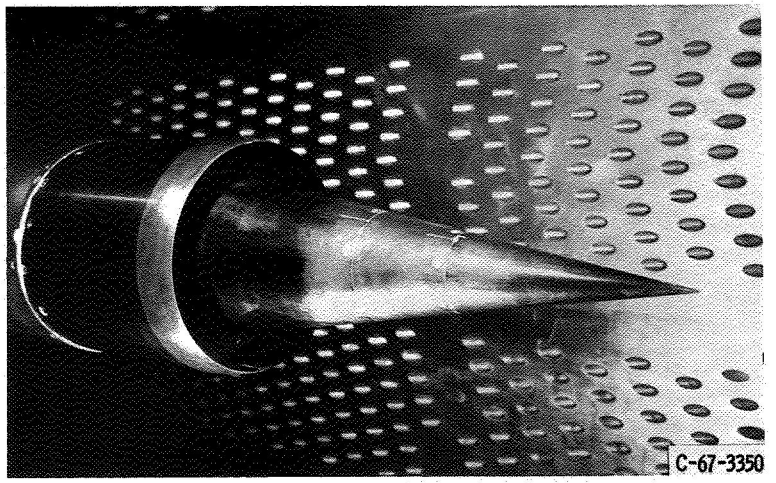

Shroud location: x/d, 0.515; A_9/A_8, 1.92

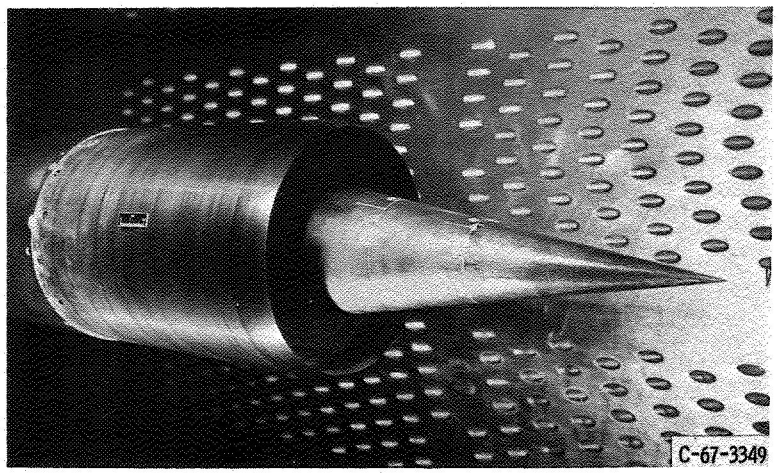

Shroud location: x/d, 0.915; A_9/A_8, 2.41

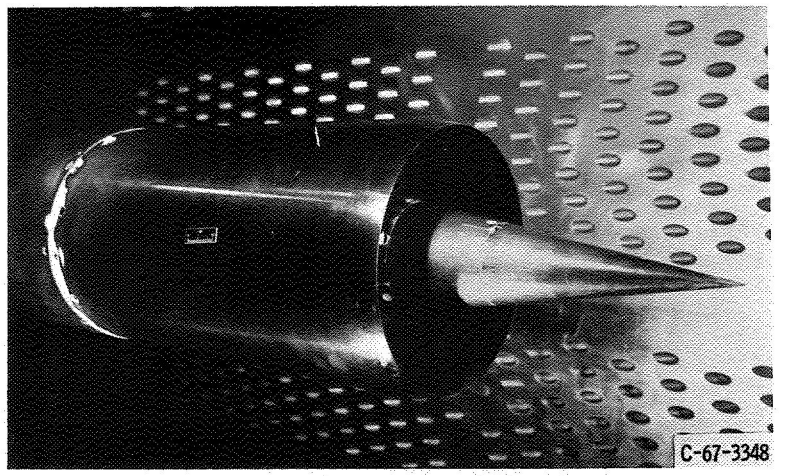

Shroud location: x/d, 1.315; A_9/A_8, 3.01

Figure 4. - Full-length plug with translating shroud. (Shroud locations are expressed in terms of axial length to diameter ratio and internal area ratio.)

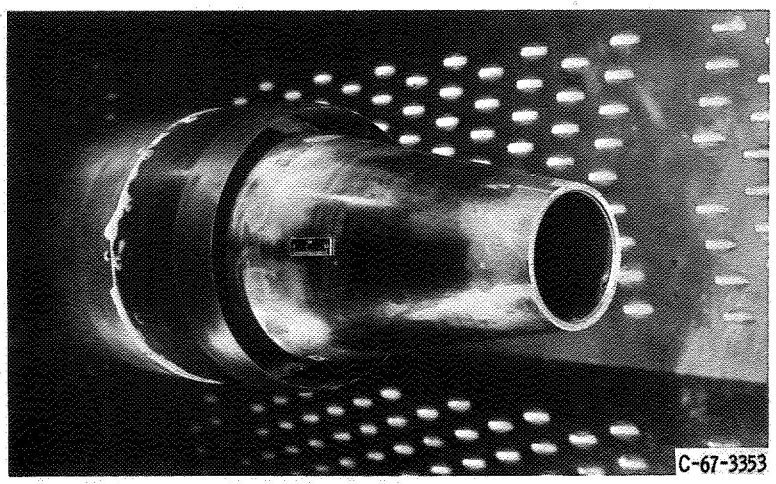

Shroud location: x/d, 0.087; A_9/A_8, 1.12

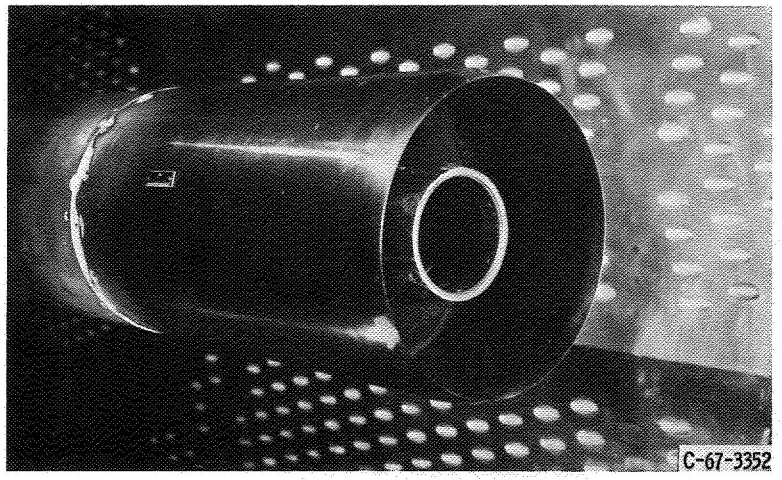

Shroud location: x/d, 1.315; A_9/A_8, 3.01 (based on full-length plug)

(a) 50 percent of plug length.

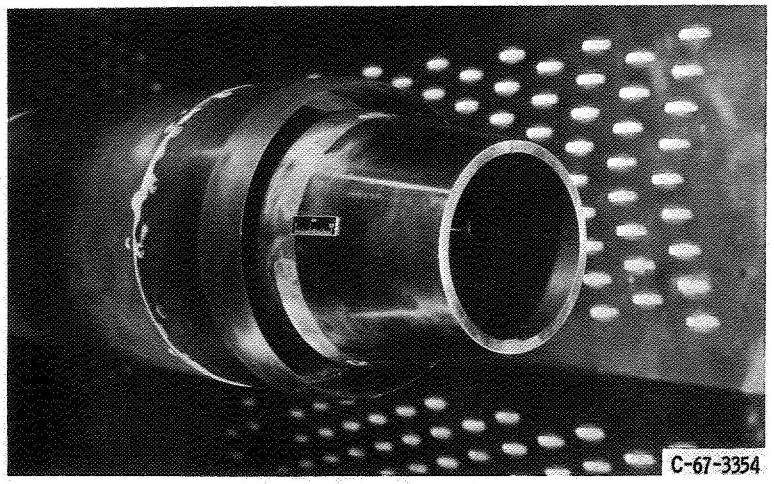

Shroud location: x/d, 0.087; A_9/A_8, 1.12

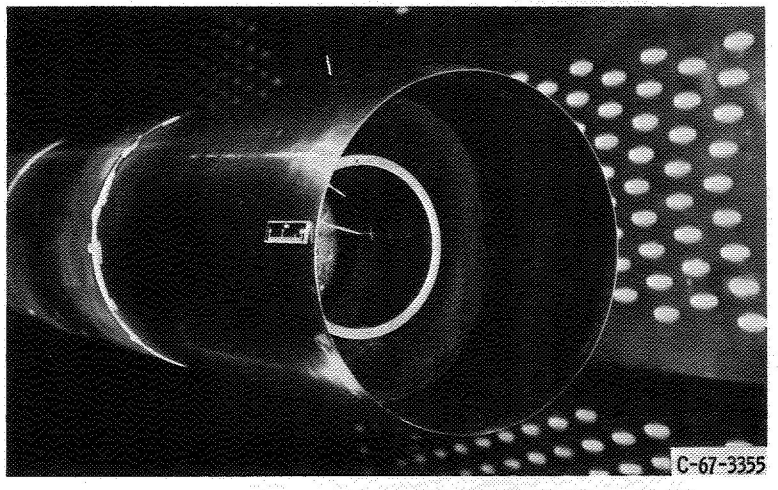

Shroud location: x/d, 1.315; A_9/A_8, 3.01 (based on full-length plug)

(b) 30 percent of plug length.

Figure 5. - Truncated plug with translating shroud. (Shroud locations are expressed in terms of axial length to diameter ratio and internal area ratio.)

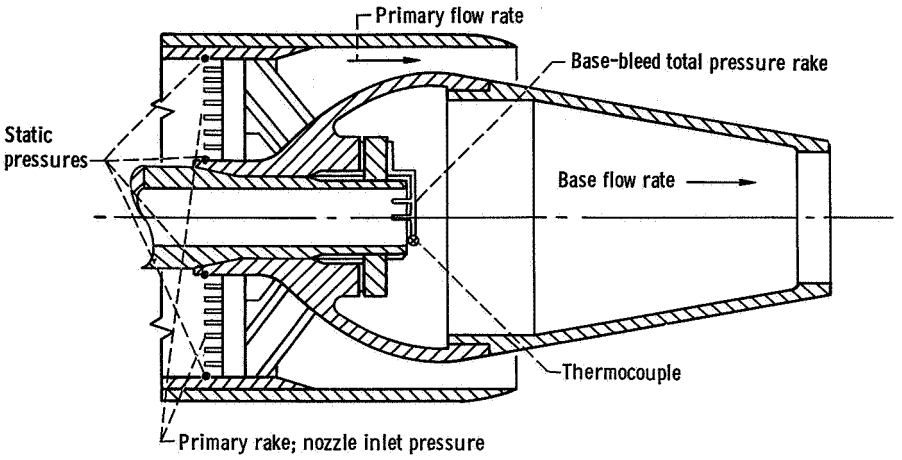

(a) Primary and base-bleed rakes.

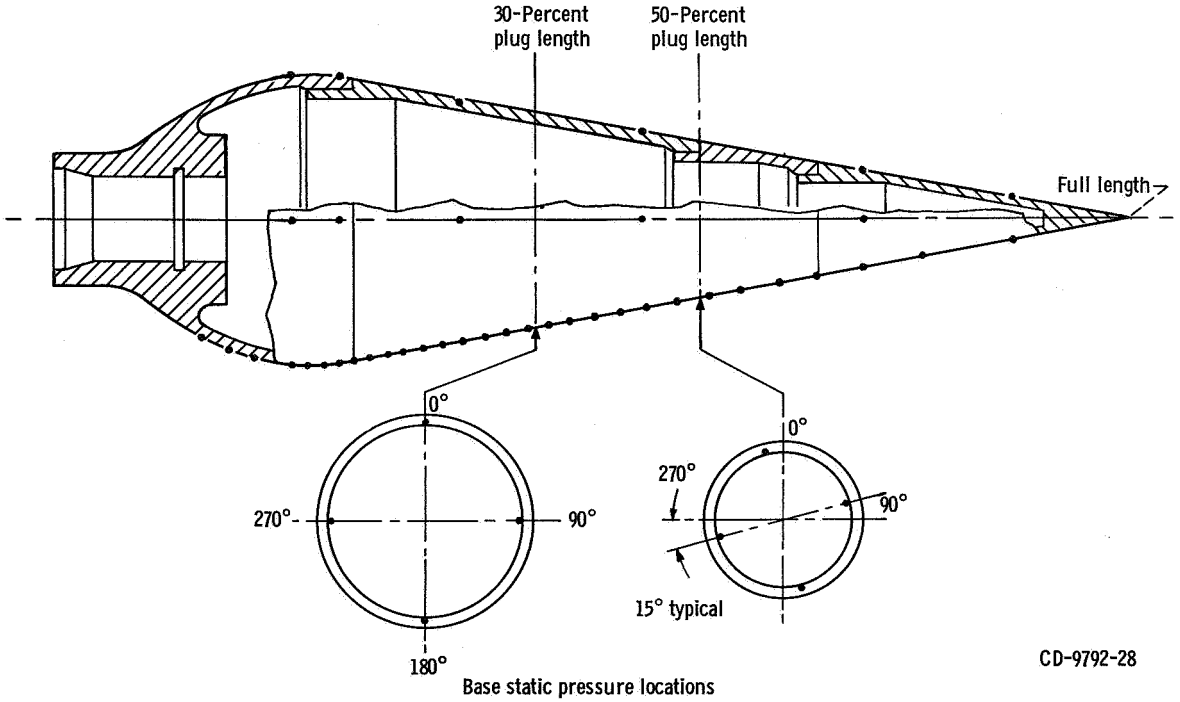

Base static pressure locations

(b) Plug static pressure locations.

Figure 6. - Model instrumentation.

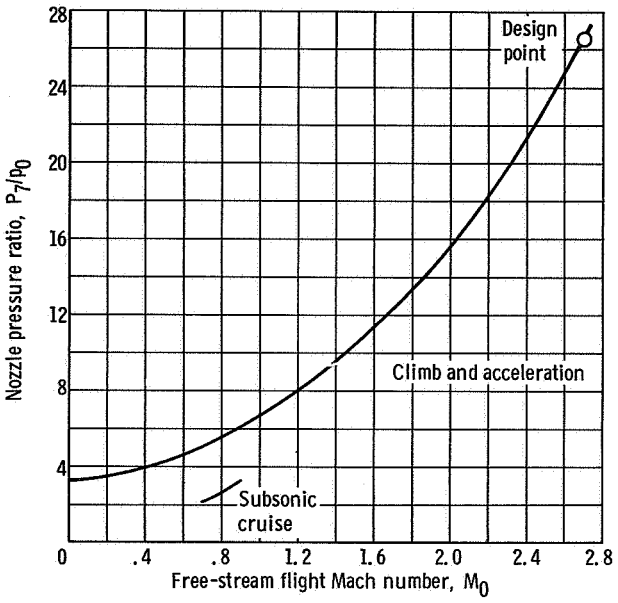

Figure 7. - Pressure ratio schedule for typical turbojet engine.

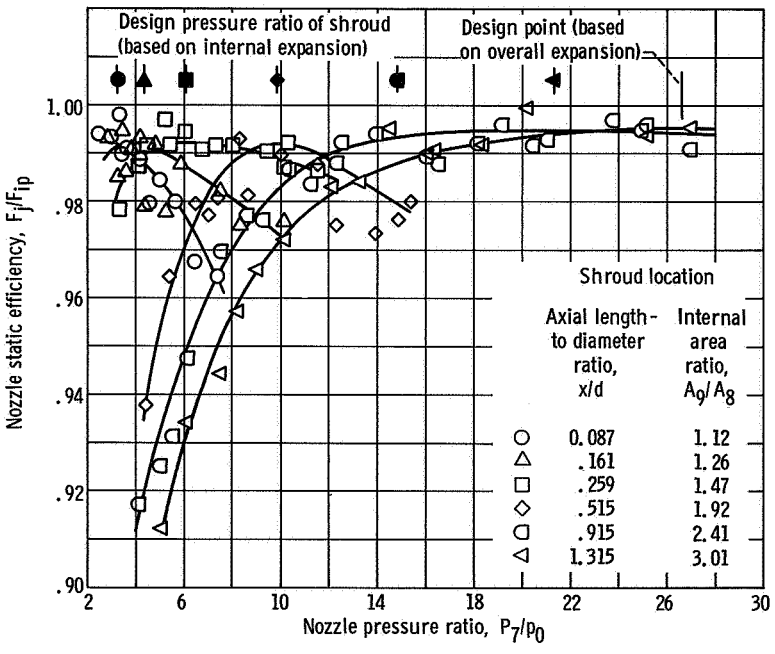

Figure 8. - Static performance of full-length plug nozzle with translating shroud.

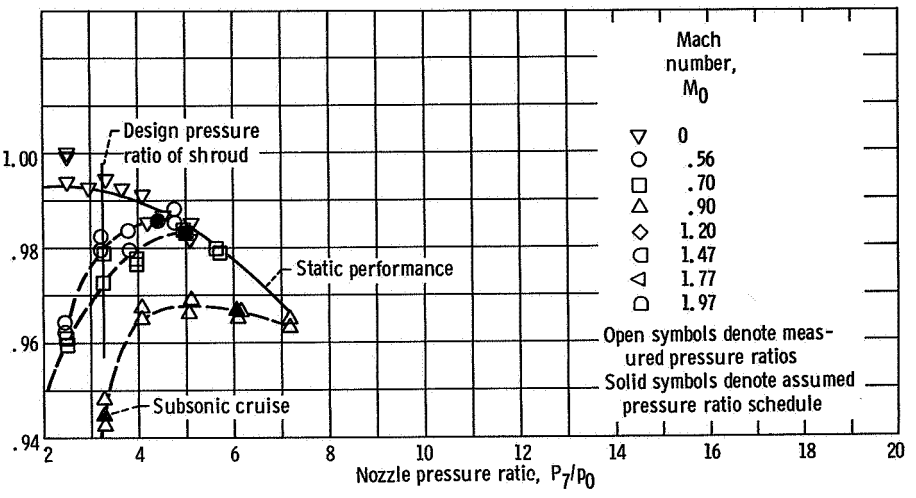

(a) Shroud location: axial length to diameter ratio, 0.087; internal area ratio, 1.12.

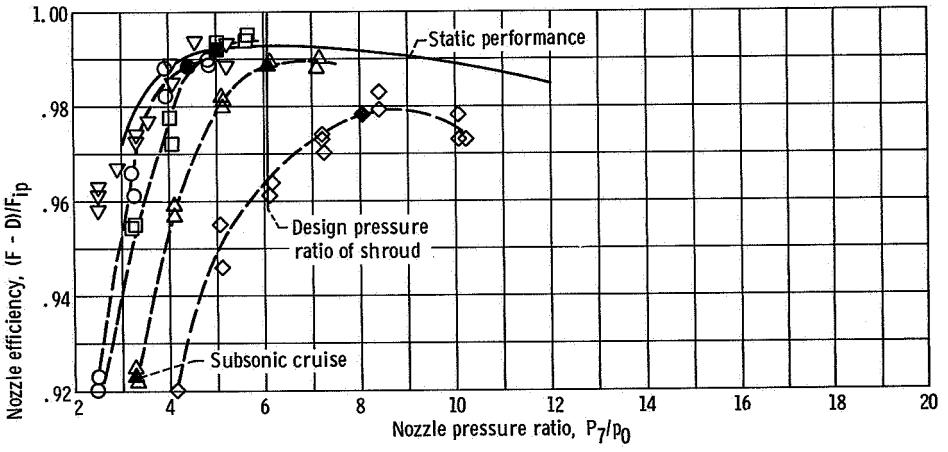

(b) Shroud location: axial length to diameter ratio, 0.259; internal area ratio, 1.47.

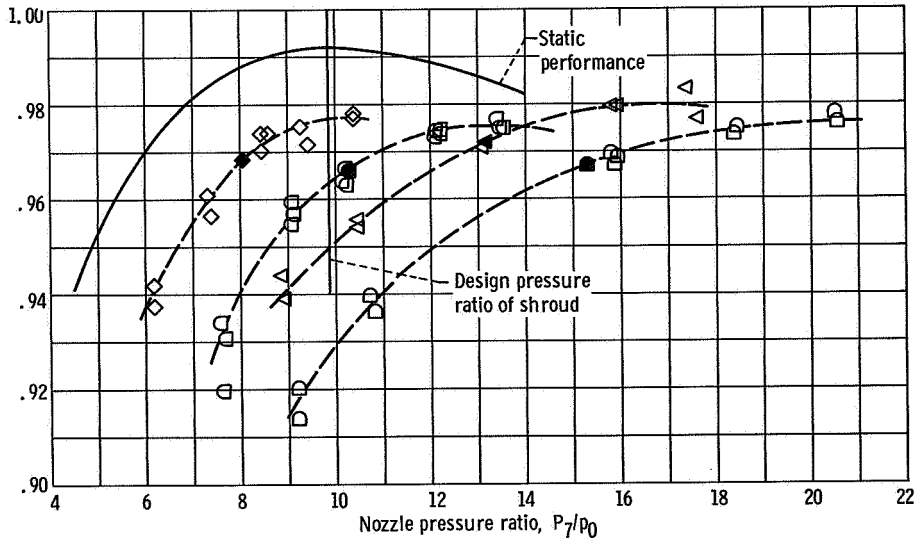

(c) Shroud location: axial length to diameter ratio, 0.515; internal area ratio, 1.92.

Figure 9. - External flow effect on full-length plug nozzle performance.

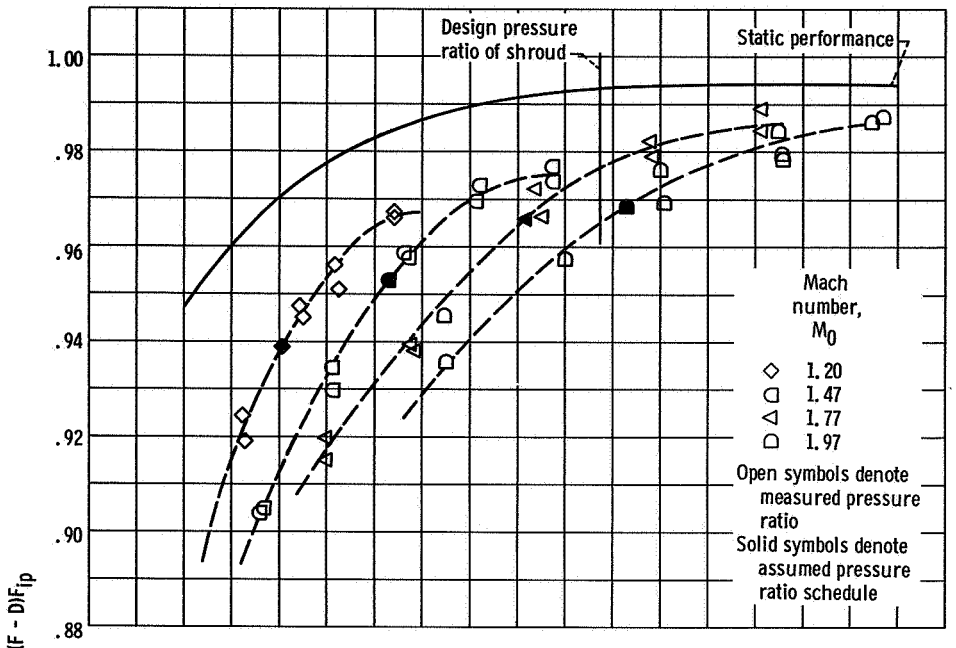

(d) Shroud location: axial length to diameter ratio, 0.915; internal area ratio, 2.41.

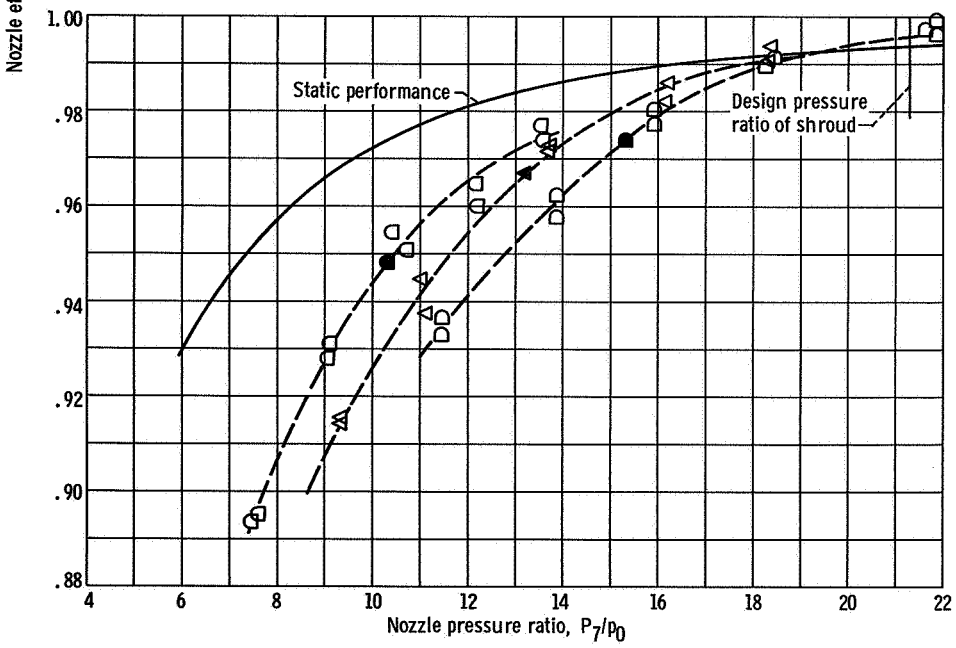

(e) Shroud location: axial length to diameter ratio, 1.315; internal area ratio, 3.01.

Figure 9. - Concluded.

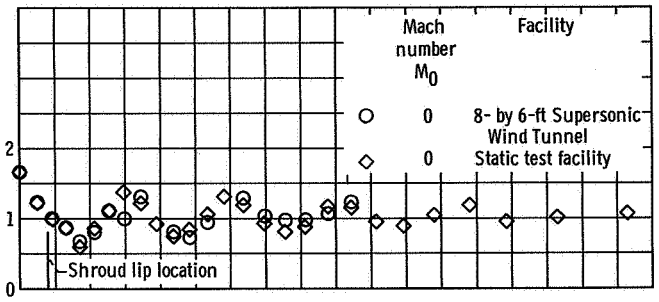

(a) Shroud location: axial length to diameter ratio, 0.087; internal area ratio, 1.12. Nozzle pressure ratio, 3.29.

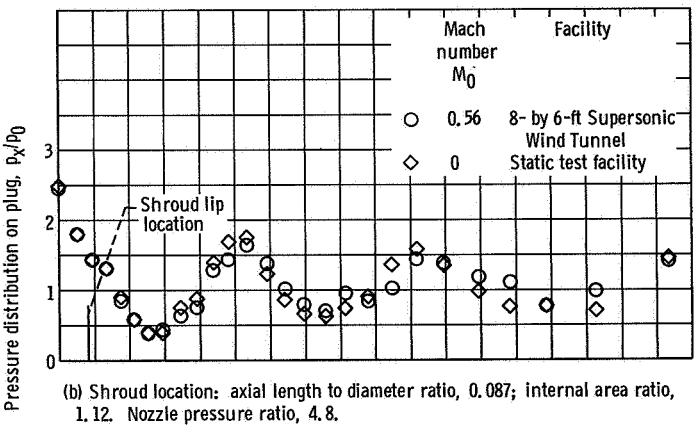

(b) Shroud location: axial length to diameter ratio, 0.087; internal area ratio, 1.12. Nozzle pressure ratio, 4.8.

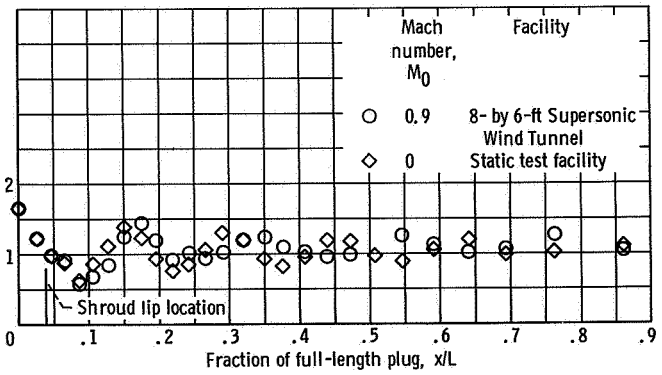

(c) Shroud location: axial length to diameter ratio, 0.087; internal area ratio, 1.12. Nozzle pressure ratio, 3.27.

Figure 10. - Effect of external flow on plug pressure distribution.

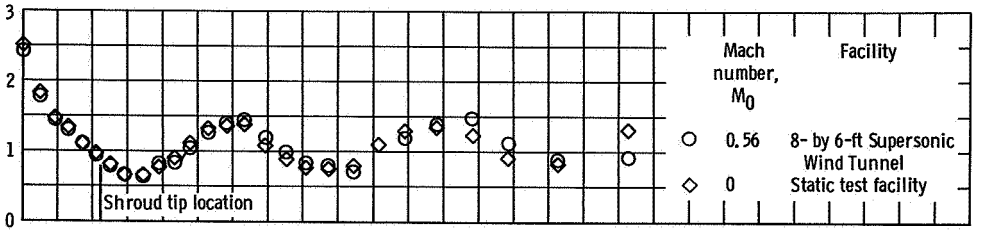

(d) Shroud location: axial length to diameter ratio, 0.259; internal area ratio, 1.47. Nozzle pressure ratio, 4.9.

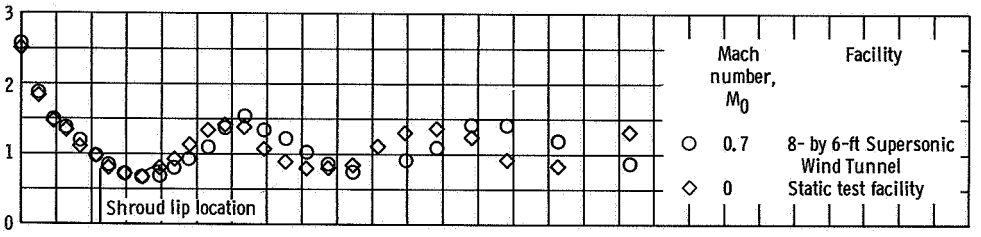

(e) Shroud location: axial length to diameter ratio, 0.259; internal area ratio, 1.47. Nozzle pressure ratio, 5.01.

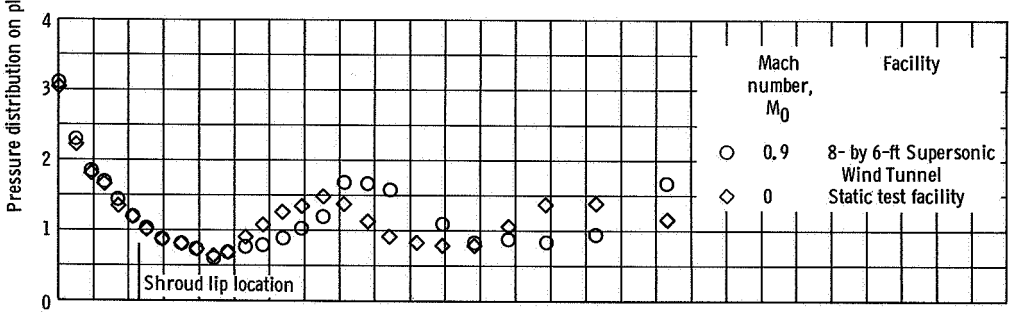

(f) Shroud location: axial length to diameter ratio, 0.259; internal area ratio, 1.47. Nozzle pressure ratio, 6.08.

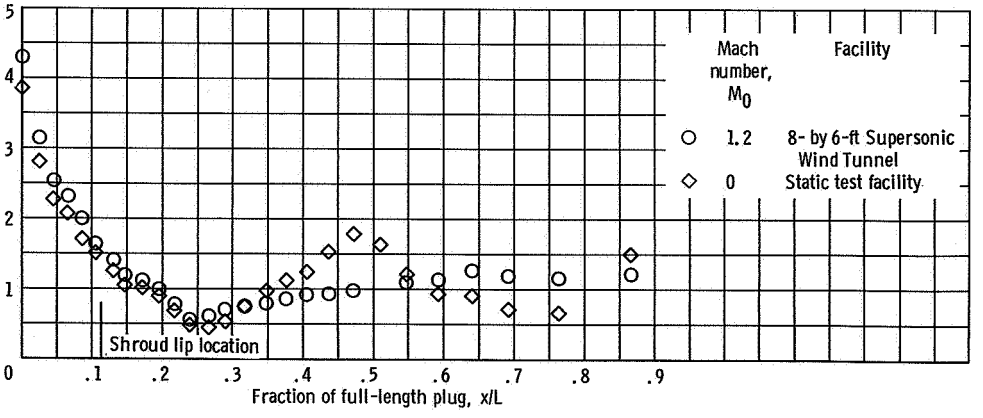

(g) Shroud location: axial length to diameter ratio, 0.259; internal area ratio, 1.47. Nozzle pressure ratio, 8.0.

Figure 10. - Continued.

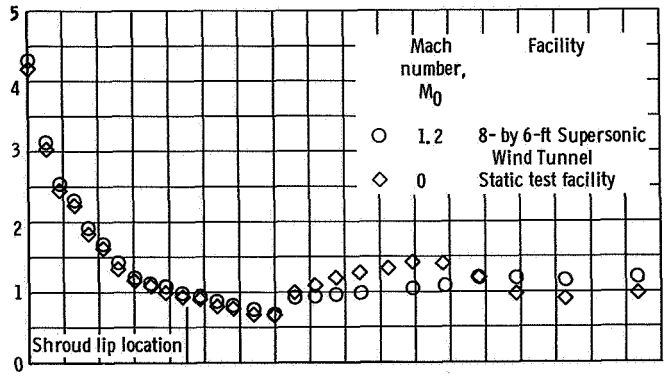

(h) Shroud location: axial length to diameter ratio, 0.515; internal area ratio, 1.92. Nozzle pressure ratio, 8.35.

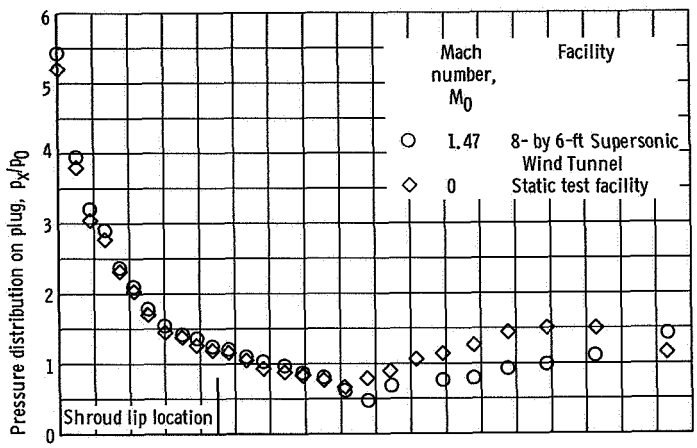

(i) Shroud location: axial length to diameter ratio, 0.515; internal area ratio, 1.92. Nozzle pressure ratio, 10.5.

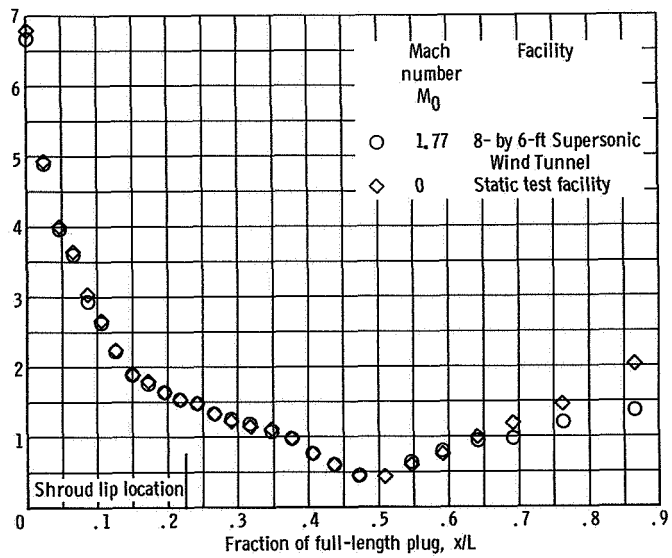

(j) Shroud location: axial length to diameter ratio, 0.515; internal area ratio, 1.92. Nozzle pressure ratio, 13.3.

Figure 10. - Continued.

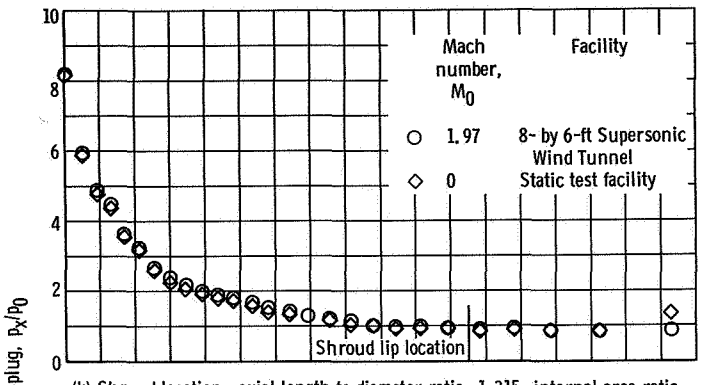

(k) Shroud location: axial length to diameter ratio, 1.315; internal area ratio, 3.01. Nozzle pressure ratio, 15.9.

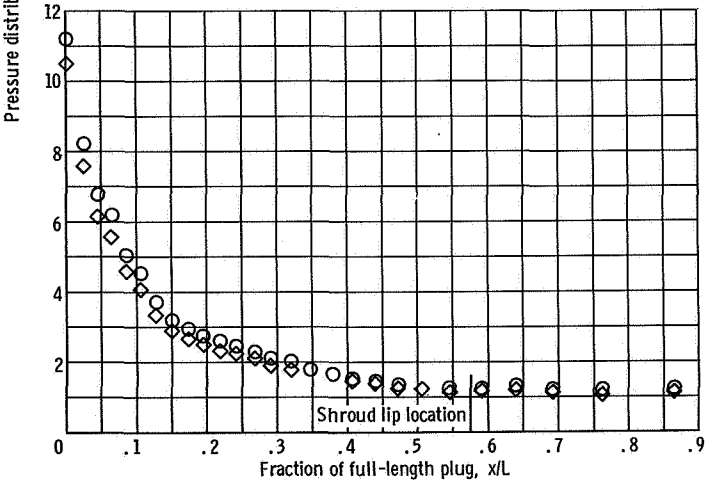

(l) Shroud location: axial length to diameter ratio, 1.315; internal area ratio, 3.01. Nozzle pressure ratio, 21.5.

Figure 10. - Concluded.

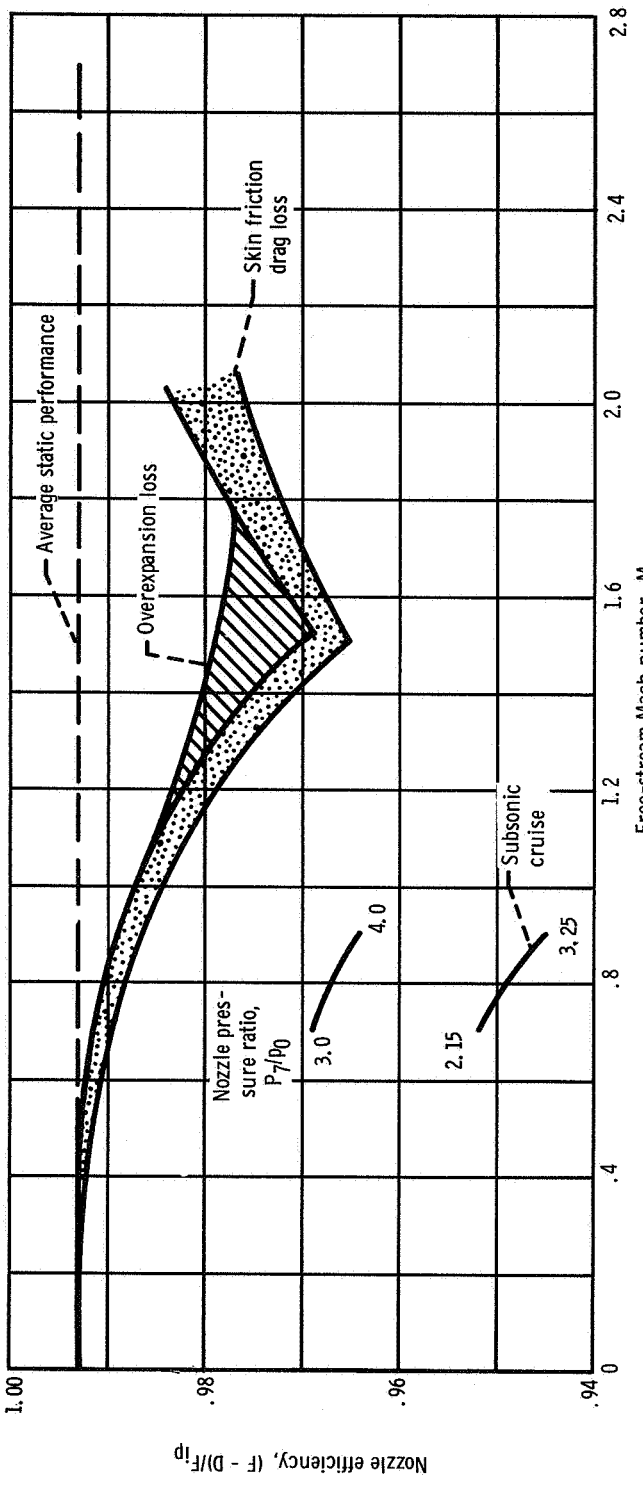

Figure 11. - Effect of external flow on full-length plug nozzle performance.

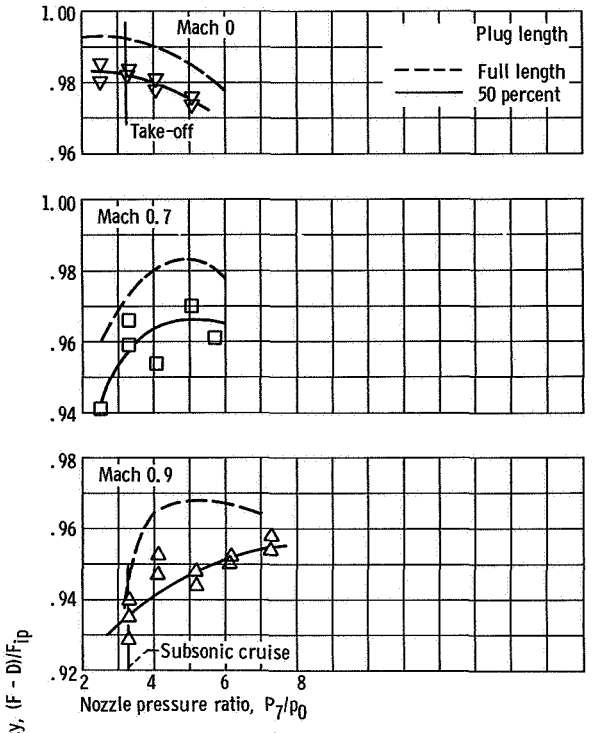

(a) Retracted shroud; axial length to diameter ratio, 0.087; internal area ratio, 1.12.

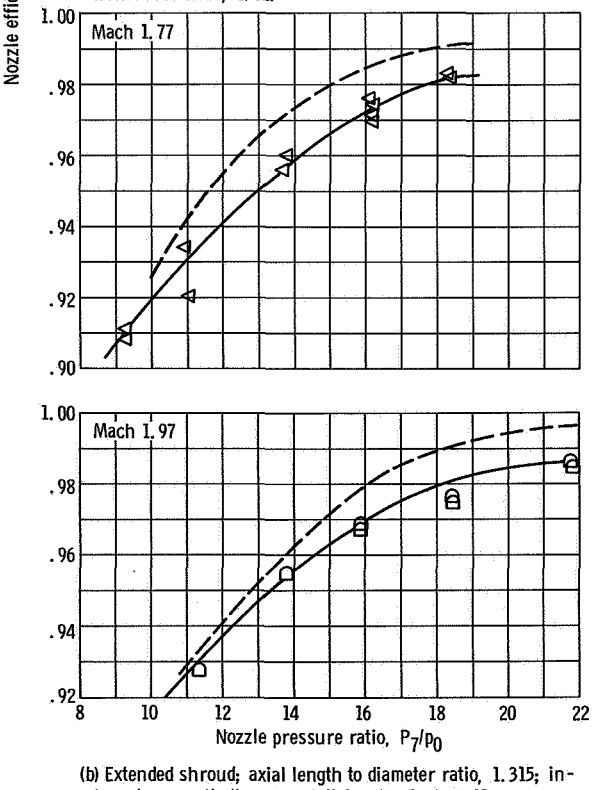

(b) Extended shroud; axial length to diameter ratio, 1.315; internal area ratio (based on full-length plug), 3.01.

Figure 12. - Nozzle performance of 50 percent plug nozzle without base bleed.

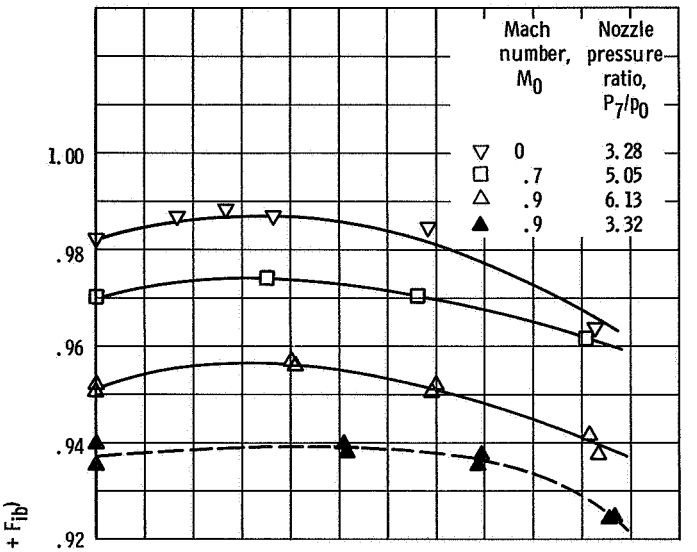

(a) Retracted shroud; axial length to diameter ratio, 0.087; internal area ratio, 1.12.

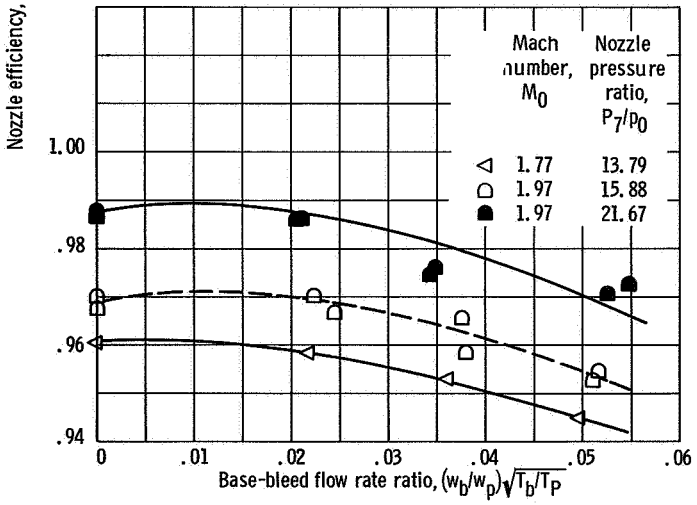

(b) Extended shroud; axial length to diameter ratio, 1.315; internal area ratio (based on full-length), 3.01.

Figure 13. - Effect of base bleed on performance of 50 percent plug nozzle.

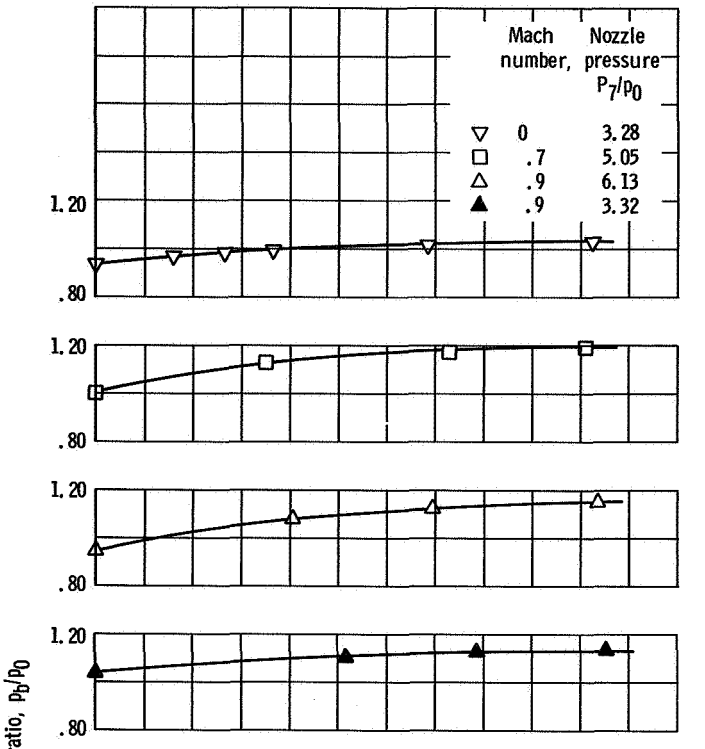

(a) Retracted shroud; axial length to diameter ratio, 0.087; internal area ratio, 1.12.

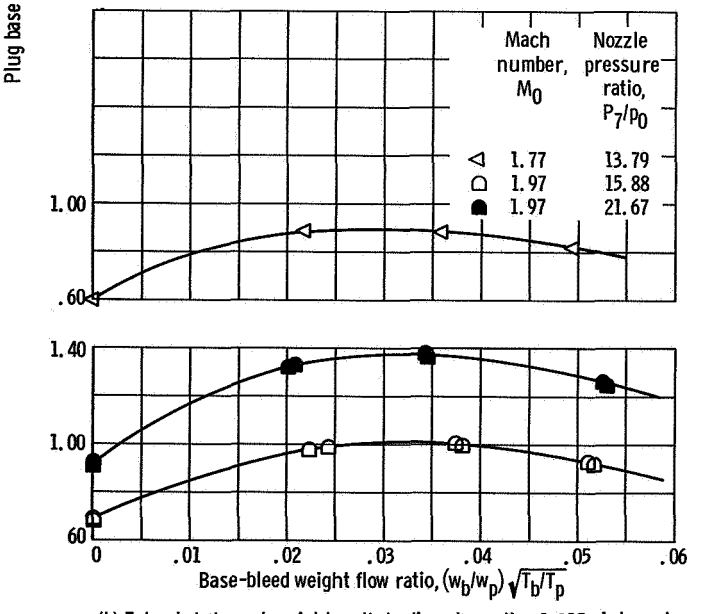

(b) Extended shroud; axial length to diameter ratio, 1.315; internal area ratio (based on full-length plug), 3.01.

Figure 14. - Effect of base bleed on base pressure for 50-percent plug nozzle.

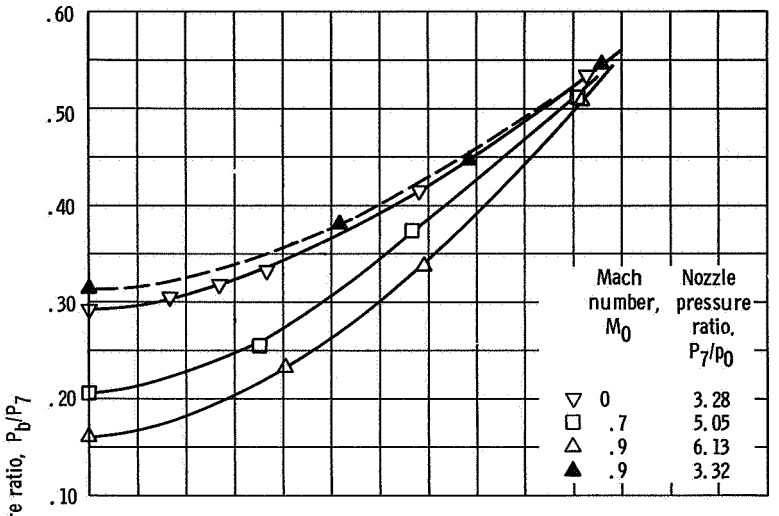

(a) Retracted shroud; axial length to diameter ratio, 0.087; internal area ratio, 1.12.

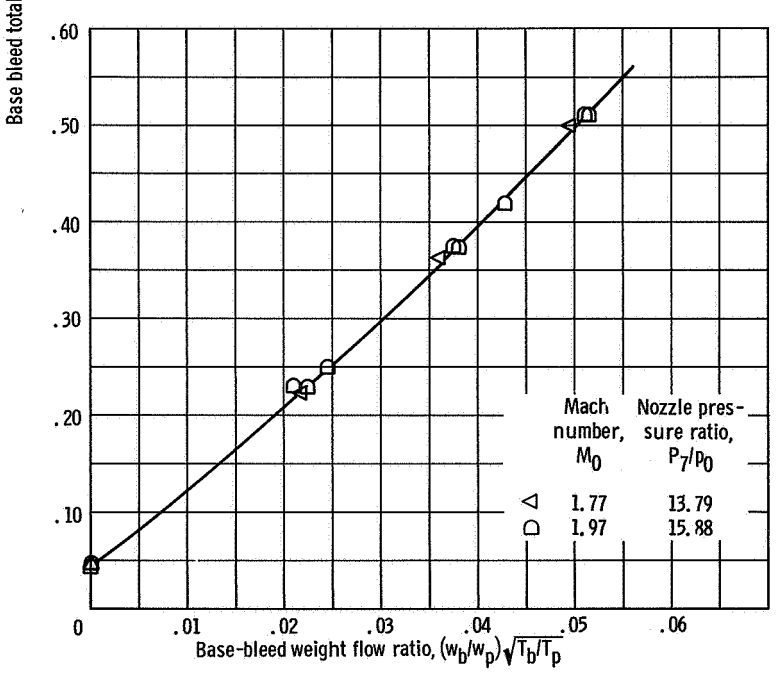

(b) Extended shroud; axial length to diameter ratio, 1.315; internal area ratio (based on full-length plug), 3.01.

Figure 15. - Pumping characteristic curves for 50-percent plug nozzle.

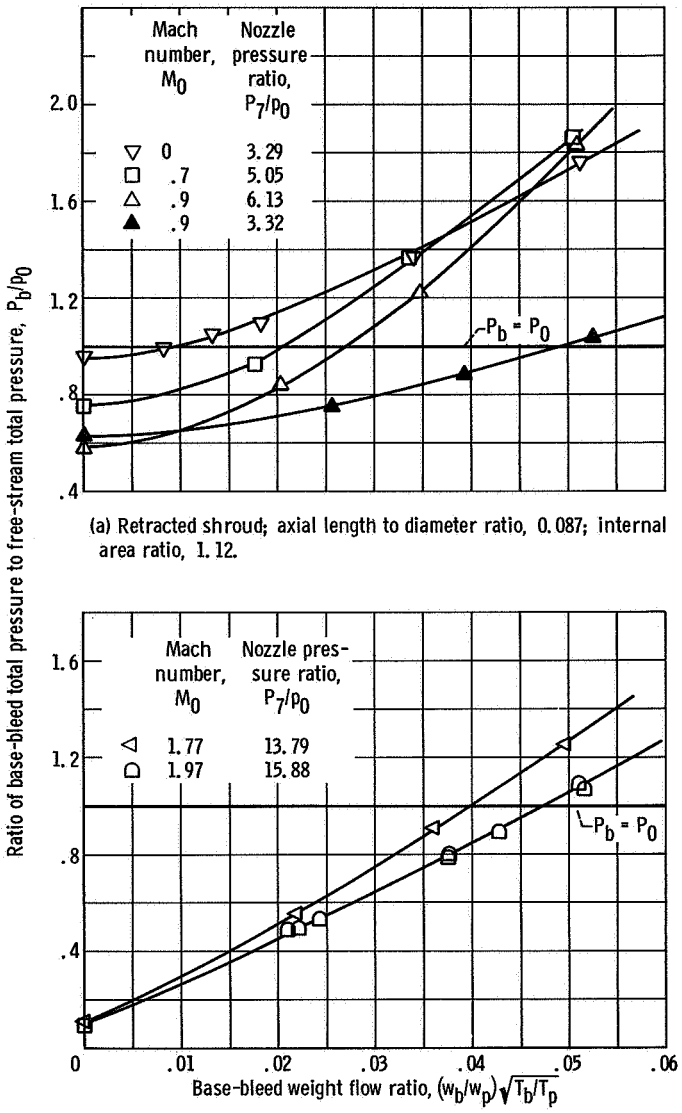

(a) Retracted shroud; axial length to diameter ratio, 0.087; internal area ratio, 1.12.

(b) Extenced shroud; axial length to diameter ratio, 1.315; internal area ratio (based on full-length plug), 3.01.

Figure 16. - Pressure recovery requirement for 50-percent plug nozzle.

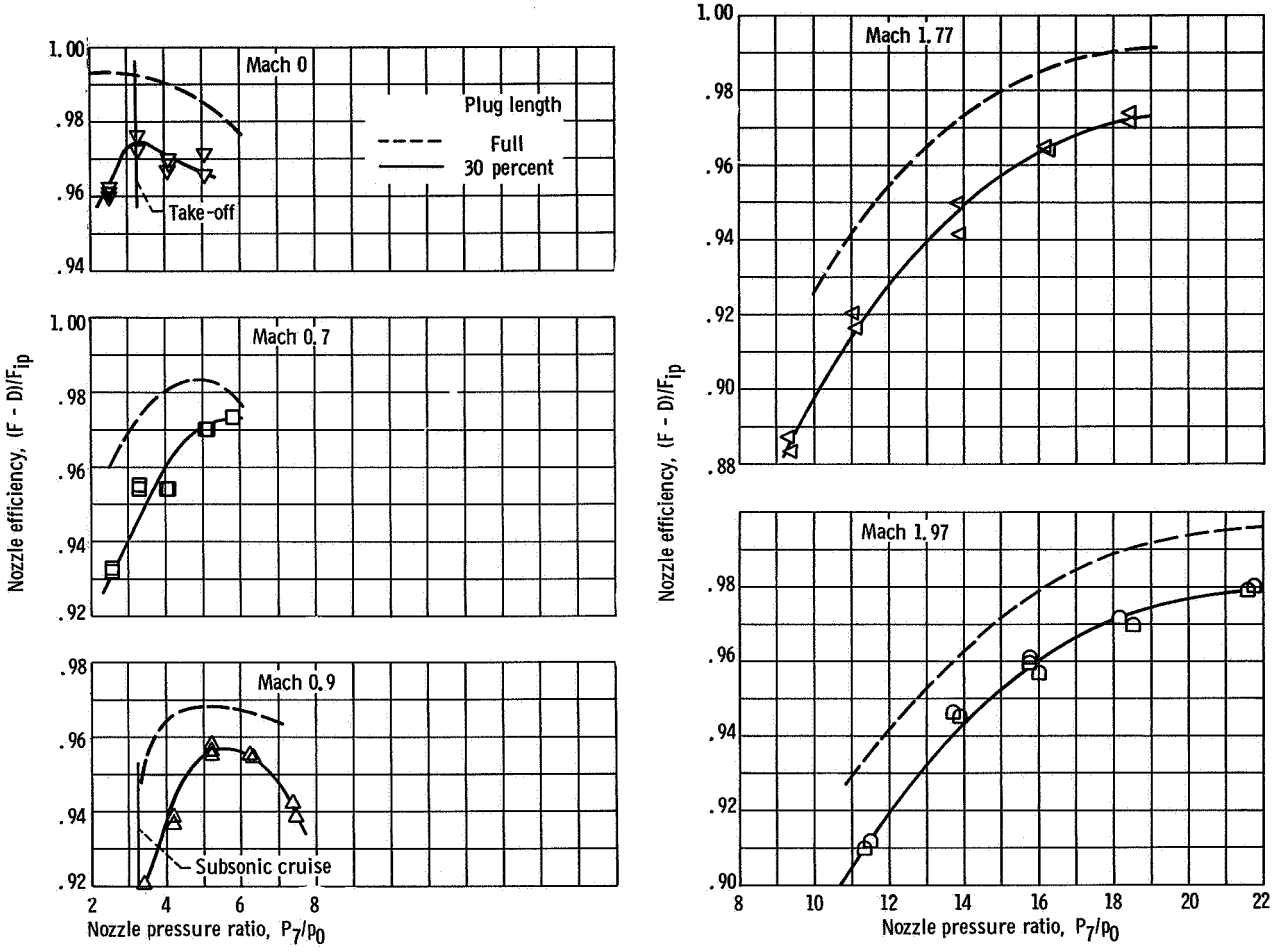

(a) Retracted shroud; axial length to diameter ratio, 0.087; internal area ratio, 1.12.

(b) Extended shroud; axial length to diameter ratio, 1.315; internal area ratio (based on full-length plug), 3.01.

Figure 17. - Nozzle performance of 30 percent plug nozzle without base bleed.

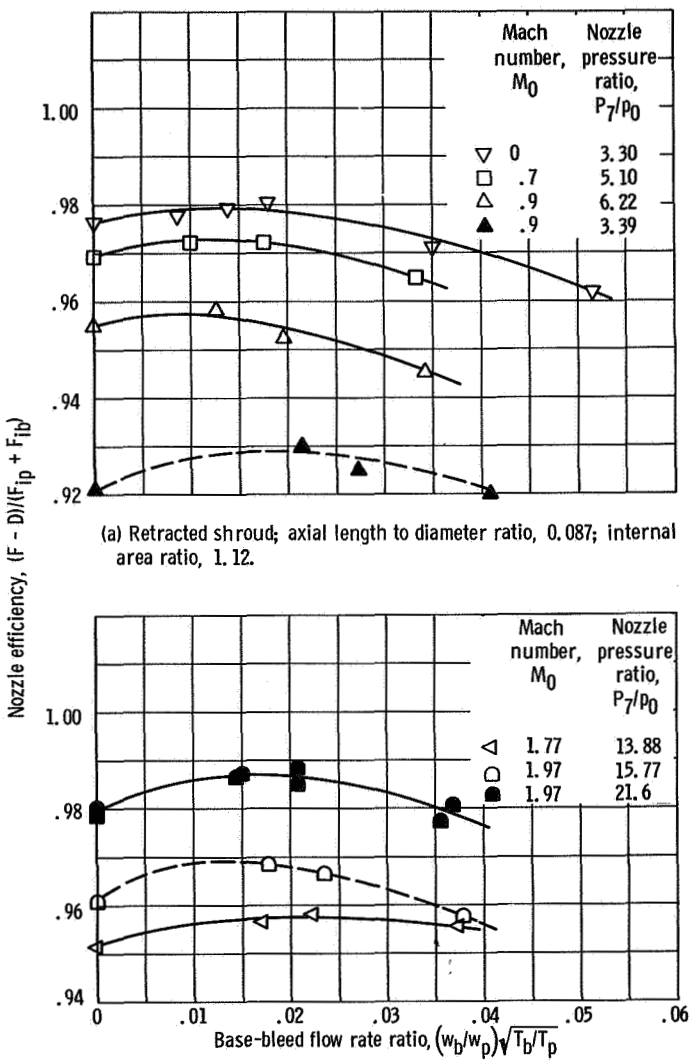

(a) Retracted shroud; axial length to diameter ratio, 0.087; internal area ratio, 1.12.

(b) Extended shroud; axial length to diameter ratio, 1.315; internal area ratio (based on full-length plug), 3.01.

Figure 18. - Effect of base bleed on performance of 30 percent plug nozzle.

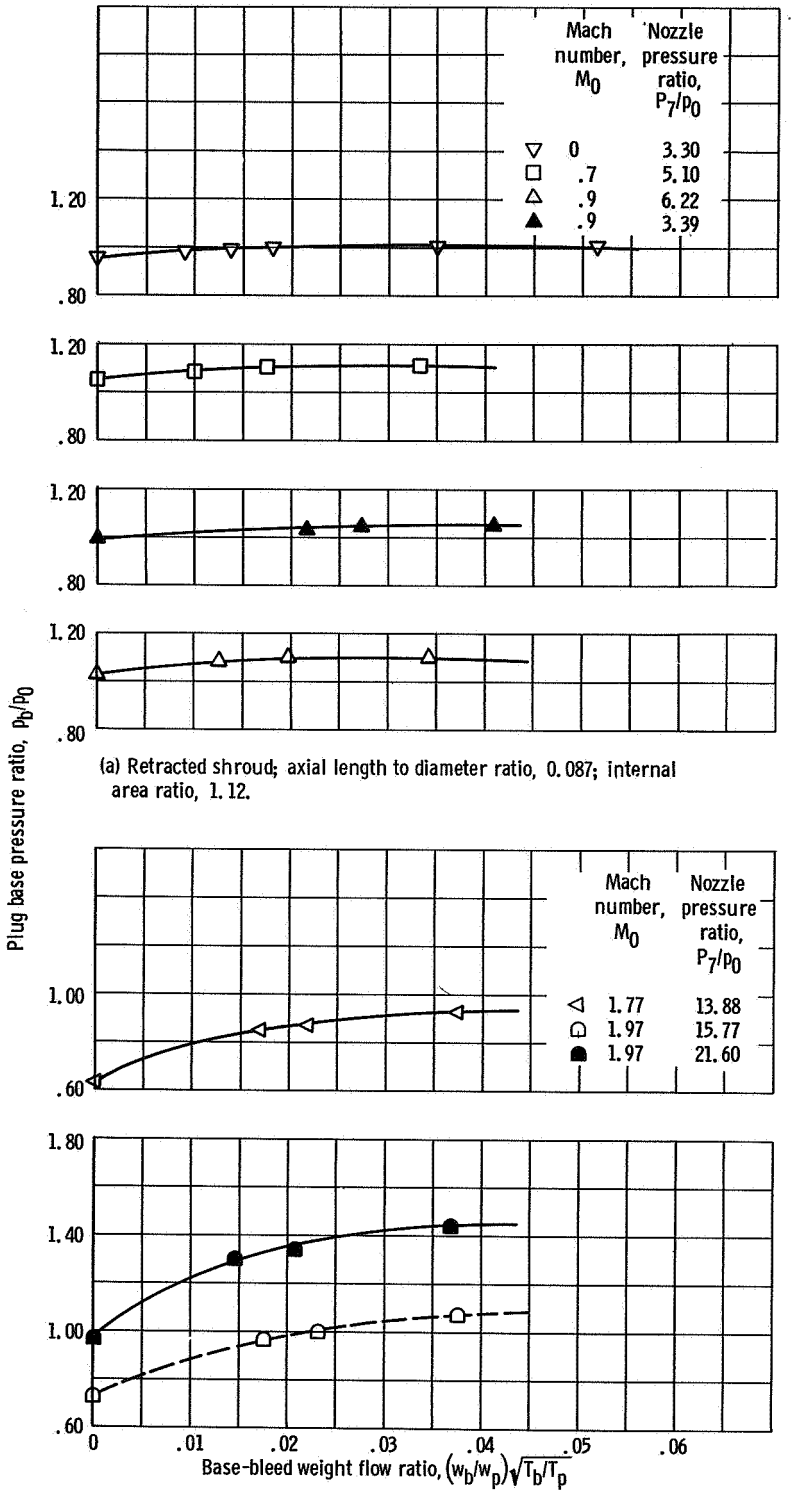

(a) Retracted shroud; axial length to diameter ratio, 0.087; internal area ratio, 1.12.

(b) Extended shroud; axial length to diameter ratio, 1.315; internal area ratio (based on full-length plug), 3.01.

Figure 19. - Effect of base bleed on base pressure for 30-percent plug nozzle.

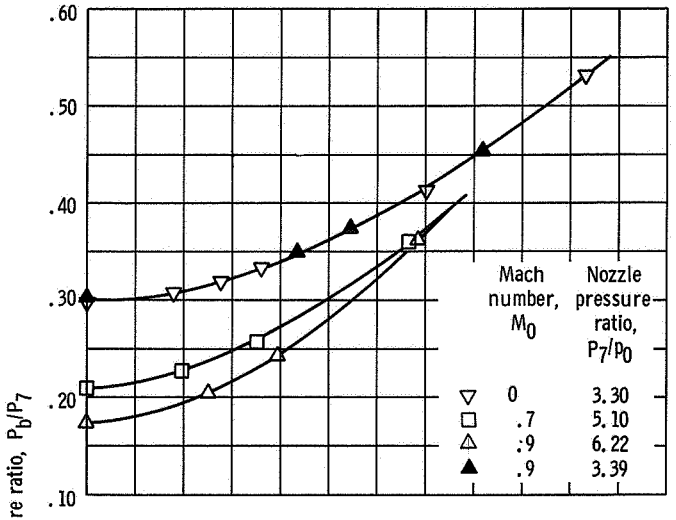

(a) Retracted shroud; axial length to diameter ratio, 0.087, internal area ratio, 1.12.

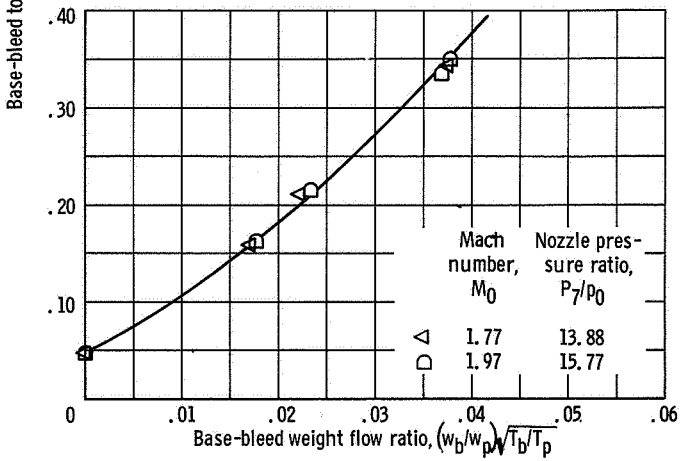

(b) Extended shroud; axial length to diameter ratio, 1.315; internal area ratio (based on full-length plug), 3.01.

Figure 20. - Pumping characteristic curves for 30-percent plug nozzle.

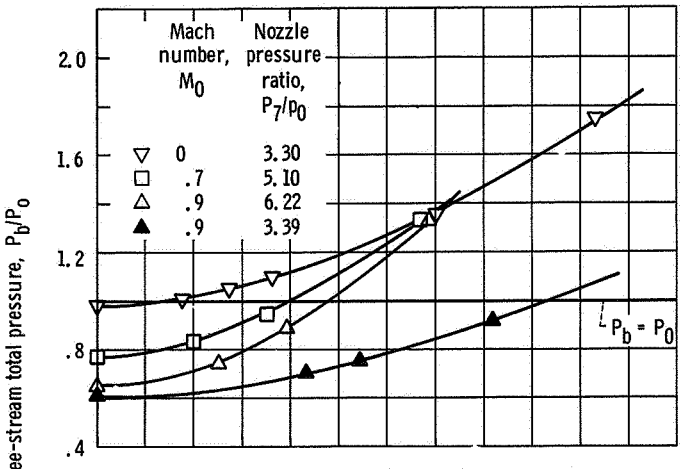

(a) Retracted shroud; axial length to diameter ratio, 0.087; internal area ratio, 1.12.

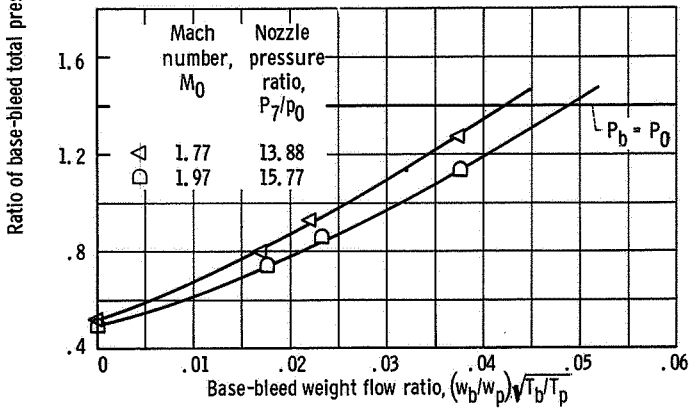

(b) Extended shroud; axial length to diameter ratio, 1.315; internal area ratio (based on full-length plug), 3.01.

Figure 21. - Pressure recovery requirement for 30-percent plug nozzle.

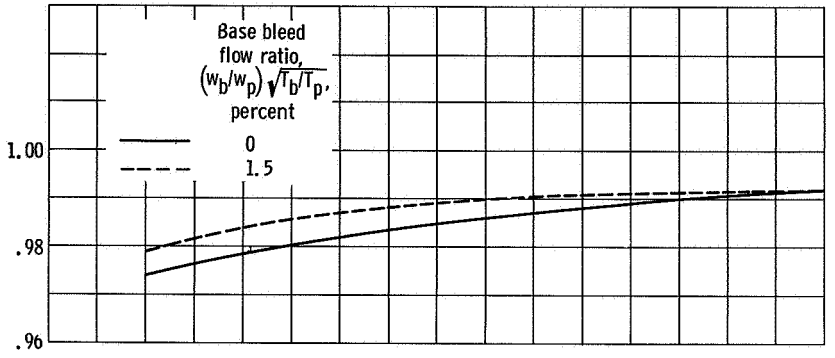

(a) Mach 0; pressure ratio, 3.25 (takeoff).

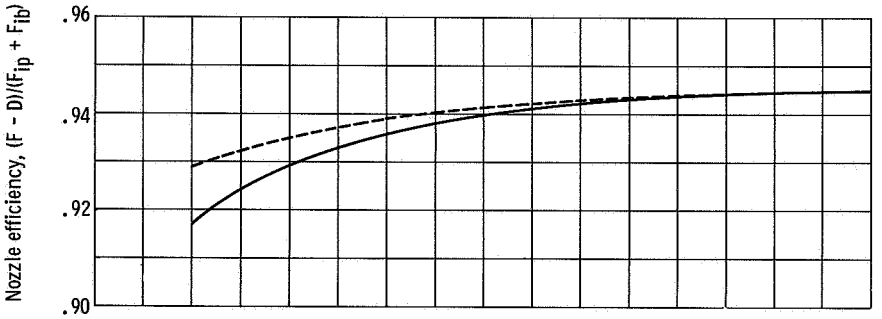

(b) Mach 0.9; pressure ratio, 3.25 (subsonic cruise).

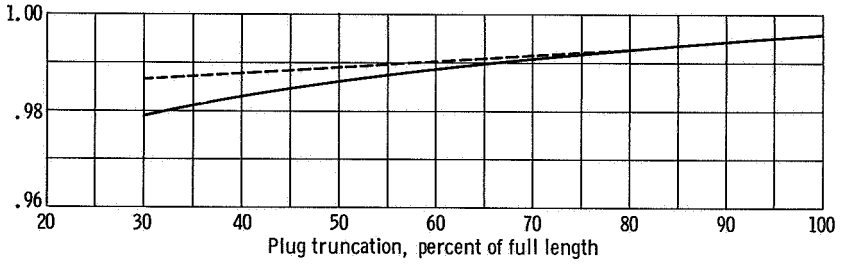

(c) Mach 1.97; pressure ratio, 22.0.

Figure 22. - Effect of plug truncation on nozzle performance.